Acta Crystallographica Section F
Structural Biology and Crystallization Communications
ISSN 1744-3091

Expression, purification, crystallization and preliminary X-ray crystallographic studies of a cold-adapted aspartate carbamoyltransferase from *Moritella profunda*

Dirk De Vos, Paco Hulpiau, Bjorn Vergauwen, Savvas N. Savvides and Jozef Van Beeumen*

Laboratorium voor Eiwitbiochemie en Eiwitengineering, Universiteit Gent, K. L. Ledeganckstraat 35, Ghent, Belgium

Correspondence e-mail: jozef.vanbeeumen@ugent.be

Received 2 December 2004
Accepted 26 January 2005
Online 12 February 2005

Aspartate carbamoyltransferase (ATCase) catalyzes the carbamoylation of the α-amino group of L-aspartate by carbamoyl phosphate (CP) to yield *N*-carbamoyl-L-aspartate and orthophosphate in the first step of *de novo* pyrimidine biosynthesis. Apart from its key role in nucleotide metabolism, the enzyme is generally regarded as a model system in the study of proteins exhibiting allosteric behaviour. Here, the successful preparation, crystallization and diffraction data collection of the ATCase from the psychrophilic bacterium *Moritella profunda* are reported. To date, there is no structural representative of a cold-adapted ATCase. The structure of *M. profunda* ATCase is thus expected to provide important insights into the molecular basis of allosteric activity at low temperatures. Furthermore, through comparisons with the recently reported structure of an extremely thermostable ATCase from *Sulfolobus acidocaldarius*, it is hoped to contribute to general principles governing protein adaptation to extreme environments. A complete native data to 2.85 Å resolution showed that the crystal belongs to space group $P3_221$, with unit-cell parameters a = 129.25, b = 129.25, c = 207.23 Å, $\alpha = \beta = 90$, $\gamma = 120^\circ$, and that it contains three catalytic and three regulatory subunits per asymmetric unit. The three-dimensional structure of the *Escherichia coli* ATCase was sufficient to solve the structure of the *M. profunda* ATCase *via* the molecular-replacement method and to obtain electron density of good quality.

1. Introduction

Aspartate carbamoyltransferase (ATCase; EC 2.1.3.2) catalyzes the carbamoylation of the α-amino group of L-aspartate by carbamoyl phosphate (CP) to yield *N*-carbamoyl-L-aspartate and orthophosphate in the first step of *de novo* pyrimidine biosynthesis. Apart from its key role in nucleotide metabolism, this enzyme is generally regarded as a model system in the study of proteins exhibiting allosteric behaviour. In this regard, the ATCase from *Escherichia coli* has been the subject of extensive structural and biochemical studies (reviewed in Allewell, 1989; Lipscomb, 1994; Helmstaedt *et al.*, 2001). The *E. coli* ATCase consists of catalytic chains encoded by the *pyrB* gene and regulatory chains encoded by the *pyrI* gene. The catalytic chains, organized into trimers (c_3), and the regulatory chains, organized into dimers (r_2), combine to form a dodecameric complex with the subunit composition $2(c_3):3(r_2)$. ATCase exists in different quaternary structures in different organisms. For example, in *Bacillus subtilis* the enzyme exists as a trimer of catalytic chains without any regulatory chains (Lerner & Switzer, 1986).

The X-ray structure of the dodecameric enzyme from *E. coli* has been determined in both the absence and presence of substrates/inhibitors/products (Kim *et al.*, 1987; Ke *et al.*, 1988; Gouaux & Lipscomb, 1988, 1990; Gouaux *et al.*, 1990; Jin *et al.*, 1999; Huang & Lipscomb, 2004). Furthermore, a low-resolution C^α trace of the *B. subtilis* enzyme is also available (Stevens *et al.*, 1991). Recently, we reported the first structure of the intact (unliganded) dodecameric ATCase from a hyperthermophilic organism (De Vos *et al.*, 2004). To date, however, the three-dimensional structure of a cold-adapted ATCase is an important missing component in our understanding of extremophilic proteins. The structure of a psychrophilic ATCase would thus lead to a better understanding of cold activity and thermolability of enzymes in general and in particular in relation to

allosteric regulation. Furthermore, structural characterization of psychrophilic enzymes may provide clues on how to improve their stability at higher temperatures while maintaining their flexibility in a colder environment, a feature that may be useful in many biotechnological applications (Gerday *et al.*, 2000).

Here, we report the successful expression, purification, crystallization and structure determination of the ATCase from *Moritella profunda*, a psychropiezophilic eubacterium isolated from deep Atlantic sediments. The *pyrB* and *pyrI* genes of *M. profunda* were isolated previously by complementation of an *E. coli pyrBI* mutant; they show sequence identities of 74 and 52%, respectively, with their *E. coli* counterparts (Xu, 2002). Based on this, tertiary and quaternary structures similar to the *E. coli* ATCase were expected for the *M. profunda* enzyme. We have now been able to determine the structure of *M. profunda* ATCase using maximum-likelihood methods as implemented in the recently launched program *PHASER* v.1.2 (Storoni *et al.*, 2004). We have identified three copies of the catalytic chain and three copies of the regulatory chain in the asymmetric unit. Model building and refinement of the structure are under way.

2. Materials and methods

2.1. Protein preparation

The cloning of the *pyrB* and *pyrI* genes of *M. profunda* by complementation of an *E. coli pyrBI* mutant has been described previously (Xu, 2002). These genes were subsequently inserted into the expression plasmids pET-Duet and pACYC-Duet (Novagen), which are designed to coexpress two target genes using separate promoters. The *pyrB* gene was cloned for production of the catalytic chain with an N-terminal 6×His tag containing the sequence MGSSHHHHHHSQDPNS. When transformed into *E. coli* BL21(DE3), both constructs resulted in substantial amounts of recombinant protein. SDS–PAGE analysis revealed that similar amounts of catalytic and regulatory chain were present. Comparison of the protein expressed in the native host with the recombinant protein shows that they display very similar functional properties (work to be published). A 10 ml volume of an overnight 301 K starter culture was inoculated into 1 l Luria–Bertani medium (Sambrook *et al.*, 1989) at the same temperature. When the culture medium reached an optical density (at 600 nm) of 0.5, isopropyl-β-D-thiogalactoside (IPTG) was added to a final concentration of 0.5 m*M*, after which the culture was incubated overnight at 288 K. The cell pellet obtained after centrifugation was resuspended in 50 m*M* Tris–HCl containing 300 m*M* NaCl at a final pH of 8.0 (buffer *A*). The cells were lysed by sonication and the cell-free supernatant was loaded onto an Ni–NTA column (Qiagen). After washing the column with buffer *A* containing 10 m*M* imidazole, the protein was eluted with buffer *A* containing 250 m*M* imidazole. The protein was then further purified to homogeneity on a Superdex-200 size-exclusion column (Amersham) and the quality of the purification was evaluated with SDS–PAGE (Fig. 1). The high NaCl concentration in buffer *A* served mainly to prevent precipitation of the recombinant ATCase on the Ni–NTA column.

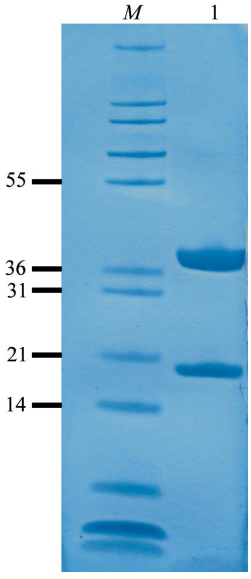

Figure 1
SDS–PAGE analysis of recombinant *M. profunda* ATCase. Lane 1, purified enzyme. Molecular standards (kDa) are indicated by *M*.

2.2. Crystallization and data collection

Owing to the temperature lability of the enzyme, all crystallization trials were performed at 277 K. Because the protein precipitates at lower temperatures, it was stored at this temperature at a concentration of 10 mg ml^{-1} in 5 m*M* Tris–HCl with 30 m*M* NaCl at a final pH of 8.0. Under these conditions, the protein is stable and retains its activity for at least six months. Crystallization experiments were performed using the hanging-drop vapour-diffusion method. Drops were prepared by mixing equal volumes of protein solution and precipitant solution and were allowed to equilibrate against 500 µl reservoir solution.

Selected crystals were transferred to a solution containing 20%(*v*/*v*) glycerol in mother liquor prior to flash-cooling by plunging directly into liquid nitrogen. From crystals tested on our in-house FR591 rotating-anode generator (Bruker–Nonius), those diffracting the best were selected for further testing with synchrotron radiation. X-ray diffraction data were collected at a wavelength of 0.92 Å at beamline BW7A (DESY, EMBL Hamburg Outstation, Germany) using a MAR CCD (MAR Research) detector system. A native data set was collected from a single crystal. The crystal-to-detector distance was 220 mm. A total of 240 rotation images were collected with an oscillation angle of 0.5°. Data processing was carried out using the programs *DENZO* and *SCALEPACK* (Otwinowski & Minor, 1997). The diffraction intensities were indexed using the program *DENZO* and were scaled and merged to 2.85 Å resolution using the program *SCALEPACK*. Intensities were converted into structure-factor amplitudes using the program *TRUNCATE* from the *CCP*4 suite (Collaborative Computational Project, Number 4, 1994).

Figure 2
Trigonal crystals of the *M. profunda* ATCase. The crystals grew as rhombohedra with typical dimensions of 0.3 × 0.3 × 0.3 mm.

Table 1
X-ray data-collection statistics.

Values in parentheses refer to the highest resolution shell.

Space group	$P3_221$
Unit-cell parameters (Å, °)	$a = b = 129.25$, $c = 207.23$, $\alpha = \beta = 90$, $\gamma = 120$
Packing density V_M (Å^3 Da^{-1})	3.1
Solvent content (%)	60.5
Resolution (Å)	50.0–2.85 (2.93–2.85)
No. of unique reflections	45685 (3817)
Redundancy	6.7 (6.8)
R_{sym}† (%)	14.9 (53.6)
Average $I/\sigma(I)$	9.9 (3.3)
Completeness (%)	96.1 (97.3)

† $R_{sym} = \sum_h \sum_i |I(h,i) - \langle I(h)\rangle| / \sum_h \sum_i I(h,i)$, where $I(h,i)$ is the intensity of the ith measurement of reflection h and $\langle I(h)\rangle$ is the average value over multiple measurements.

3. Results and discussion

From an initial screening of crystallization conditions with Structure Screen 1 (Molecular Dimensions Ltd), five conditions were found that produced crystals (conditions 27, 30, 32, 44 and 45). Except for condition 45 (4.0 *M* sodium formate), all other conditions contained lithium or ammonium sulfate as the precipitant. Starting from condition 32 (0.1 *M* Tris pH 8.5, 2.0 *M* ammonium sulfate), the buffer pH and precipitant concentration were optimized. Lowering the ammonium sulfate concentration to 1.5 *M* was sufficient to provide crystals that grew overnight to dimensions of 0.3 × 0.3 × 0.3 mm (Fig. 2). Crystals could be obtained within the pH range 7.0–8.5 and their quality did not vary in a pH-dependent manner. The relative ease with which the *M. profunda* ATCase crystallizes challenges the general notion that cold-adapted proteins are difficult to crystallize because of inherent flexibility. Similar cases have been reported in the past (Villeret *et al.*, 1997; Van Petegem *et al.*, 2002).

A complete data set was collected to 2.85 Å resolution using a single crystal grown at pH 8.0. The full data-collection statistics are presented in Table 1. Assuming a subunit molecular weight for the catalytic and regulatory chains of 36 152 and 16 889 Da, respectively, and assuming three copies of each chain in the asymmetric unit, the solvent content of the crystal was 60.5%, with a volume-to-weight ratio of 3.1 Å^3 Da^{-1}. These values are within the frequently observed ranges for protein crystals (Matthews, 1968).

One subunit of the *E. coli* ATCase catalytic chain (Stevens *et al.*, 1990; PDB code 6at1) served as the starting model for solving the structure by molecular replacement using maximum-likelihood methods implemented in the program *PHASER* v.1.2 (Storoni *et al.*, 2004). In a fully automated rotational and translational search, three copies of the catalytic chain with reasonable packing could be located in the asymmetric unit. Three copies of the smaller regulatory subunits could also be located. This was performed by refeeding *PHASER* with the catalytic chain after a first round of model refinement and searching with the *E. coli* ATCase regulatory chain (PDB code 6at1). Furthermore, we were able to resolve the ambiguity between the enantiomorphic space groups $P3_121$ and $P3_221$ in favour of the second. After applying the crystallographic symmetry operations of space group $P3_221$, we found that the positions of the catalytic and regulatory chains correspond well with their position in the *E. coli* ATCase dodecameric complex. Combining this with the result from size-exclusion chromatography and with our finding that the regulatory chains were co-purified on Ni–NTA in equal amounts with the histidine-tagged catalytic chains suggests that the *M. profunda* ATCase quaternary organization is in agreement with that of *E. coli*, *i.e.* $2(c_3):3(r_2)$. Initial electron-density maps revealed several unique structural features of *M. profunda* ATCase compared with the search models and thus confirmed the correctness of our solution. Model building and refinement of this structure are under way.

We gratefully acknowledge access to EMBL beamline BW7A at the DORIS storage ring, DESY, Hamburg. DDV is a Research Fellow of the Research Foundation-Flanders (FWO-Vlaanderen).

References

Allewell, N. M. (1989). *Annu. Rev. Biophys. Chem.* **18**, 71–92.
Collaborative Computational Project, Number 4 (1994). *Acta Cryst.* D**50**, 760–763.
De Vos, D., Van Petegem, F., Remaut, H., Legrain, C., Glansdorff, N. & Van Beeumen, J. J. (2004). *J. Mol. Biol.* **339**, 887–900.
Gerday, C., Aittaleb, M., Bentahir, M., Chessa, J. P., Claverie, P., Collins, T., D'Amico, S., Dumont, J., Garsoux, G., Georlette, D., Hoyoux, A., Lonhienne, T., Meuwis, M. A. & Feller, G. (2000). *Trends Biotechnol.* **18**, 103–107.
Gouaux, J. E. & Lipscomb, W. N. (1988). *Proc. Natl Acad. Sci. USA*, **85**, 4205–4208.
Gouaux, J. E. & Lipscomb, W. N. (1990). *Biochemistry*, **29**, 389–402.
Gouaux, J. E., Stevens, R. C. & Lipscomb, W. N. (1990). *Biochemistry*, **29**, 7702–7715.
Helmstaedt, K., Krappmann, S. & Braus, G. H. (2001). *Microbiol. Mol. Biol. Rev.* **65**, 404–421.
Huang, J. & Lipscomb, W. N. (2004). *Biochemistry*, **43**, 6422–6426.
Jin, L., Stec, B., Lipscomb, W. N. & Kantrowitz, E. R. (1999). *Proteins Struct. Funct. Genet.* **37**, 729–742.
Ke, H.-M., Lipscomb, W. N., Cho, Y. & Honzatko, R. B. (1988). *J. Mol. Biol.* **204**, 725–747.
Kim, K. H., Pan, Z., Honzatko, R. B., Ke, H.-M. & Lipscomb, W. N. (1987). *J. Mol. Biol.* **196**, 853–875.
Lerner, C. G. & Switzer, R. L. (1986). *J. Biol. Chem.* **261**, 11156–11165.
Lipscomb, W. N. (1994). *Adv. Enzymol.* **68**, 67–152.
Matthews, B. W. (1968). *J. Mol. Biol.* **33**, 491–497.
Otwinowski, Z. & Minor, W. (1997). *Methods Enzymol.* **276**, 307–326.
Sambrook, J., Fritsch, E. F. & Maniatis, T. (1989). *Molecular Cloning. A Laboratory Manual*, 2nd ed. New York: Cold Spring Harbor Laboratory Press.
Stevens, R. C., Gouaux, J. E. & Lipscomb, W. N. (1990). *Biochemistry*, **29**, 7691–7701.
Stevens, R. C., Reinisch, K. M. & Lipscomb, W. N. (1991). *Proc. Natl Acad. Sci. USA*, **88**, 6087–6091.
Storoni, L. C., McCoy, A. J. & Read, R. J. (2004). *Acta Cryst.* D**60**, 432–438.
Van Petegem, F., Collins, T., Meuwis, M.-A., Gerday, C., Feller, G. & Van Beeumen, J. (2002). *Acta Cryst.* D**58**, 1494–1496.
Villeret, V., Chessa, J. P., Gerday, C. & Van Beeumen, J. (1997). *Protein Sci.* **6**, 2462–2464.
Xu, Y. (2002). PhD thesis. Vrije Universiteit Brussel, Brussels, Belgium.